


Article

# Production of Aerated Foamed Concrete with Industrial Waste from the Gems and Jewels Sector of Rio Grande do Sul-Brazil

Rudimar Pedro <sup>1</sup> , Rejane M. C. Tubino <sup>1</sup>, Jonas Anversa <sup>2</sup>, Denisar De Col <sup>2</sup>,  
Richard Thomas Lermen <sup>2</sup> and Rodrigo de Almeida Silva <sup>2,\*</sup>

<sup>1</sup> Laboratory of Environmental Studies for Metallurgy (LEAMet), Post-Graduation Program in Mining, Metallurgical and Materials Engineering (PPGE3M), Department of Engineering, Federal University of Rio Grande do Sul (UFRGS), Porto Alegre, Rio Grande do Sul 90130-120, Brazil; rudimarpedro@yahoo.com.br (R.P.); rejane.tubino@ufrgs.br (R.M.C.T.)

<sup>2</sup> Post-Graduation Program in Civil Engineering (PPGEC), Department of Civil Engineering, Polytechnic School, Meridional College (IMED), Passo Fundo, Rio Grande do Sul 99070-220, Brazil; jonas.anv@gmail.com (J.A.); denisar\_d@hotmail.com (D.D.C.); richard.lermen@imed.edu.br (R.T.L.)

\* Correspondence: rodrigo.silva@imed.edu.br; Tel.: +55-54-3045-9046

Received: 29 August 2017; Accepted: 21 September 2017; Published: 26 September 2017

**Abstract:** The use of solid waste for the development of new building materials has been an alternative to reduce environmental impacts through the preservation of natural resources. In this context, this paper evaluates the possibility of using agate gemstone waste, called rolled powder, which basically consists of silica (SiO<sub>2</sub>), in the manufacture of aerated foamed concrete blocks completely replacing the natural sand. Preformed foam was used as the air entrained by mechanical stirring with a mixture of natural foaming agents derived from coconut. To produce test specimens, the water/cement ratio and foam concentrations were varied, with three and four levels, respectively. The specimens were left for 28 days at room temperature to be cured, and then underwent analysis to determine their compressive strength, density, and the distribution of air-voids. The experiments demonstrated that the best water/cement ratio was 1.28 for 18% (of total solid mass) addition of foam, which generated a sample with a density of 430 kg/m<sup>3</sup>, and a compressive strength of 1.07 MPa. The result for compressive strength is 11% smaller than the requirements of the Brazilian standard (NBR 13438) for autoclaved aerated concrete blocks, but the results are promising.

**Keywords:** agate waste; foaming agent; aerated concrete block

## 1. Introduction

The state of Rio Grande do Sul, located in the south of Brazil, stands out nationally and internationally for its wealth of precious stones, such as agate and amethyst, which are exported to several countries in the world. According to Tubino and Sampaio [1], the state is recognized as the world's largest producer of raw agate [2]. The town of Soledade/Rio Grande do Sul (RS) was a pioneer in extracting, processing, and commercializing precious stones. Currently, it has only one industrial and commercial area of gemological asset, which accounts for a large part of its economy; 71% of companies in this area are exporters [3].

Brazilian agate and amethyst run through deposits of the "basalt geode" type [4,5], and have been crystallized in the cavities of the volcanic rocks of the Serra Geral Formation, with their diameter varying from 0.1 to 1.0 m. The geodes are filled with minerals that are formed based on a colloidal silica system [6]. Other minerals are found in these deposits, such as quartz, rock crystal, rosy quartz, calcite, apophyllite, zeolites, onyx, jasper, opal, gypsite, and barite. Brum [7] identified that the agate coming from these deposits is formed by granular and fibrous microcrystalline quartz, known as chalcedony.

In the industrial processing of gems, a substantial amount of solid waste is generated, such as fragments of agate, mud with oil, agate powder without oil, and wastewater containing dyes and metals, aside from semi-finished parts that have defects in their formation or impurities and have no commercial value [8–10].

The “Rolled Stone” (Figure 1a) is generated through agate processing and gives a round shape to the agate fragments through a ball bearing drum device (Figure 1b). In the rolling process of agate, Petry [11] estimates that about 30 tons per month of ground agate powder, known as “Rolled Powder (RP)” (Figure 1c), are produced in local industries. The RP is comprised of approximately 98% SiO<sub>2</sub> with 95% of the particles that have a diameter less than 74 μm. It can be estimated that for each kilogram of final product, 0.65 kg of agate powder is generated by the rolling process [9].

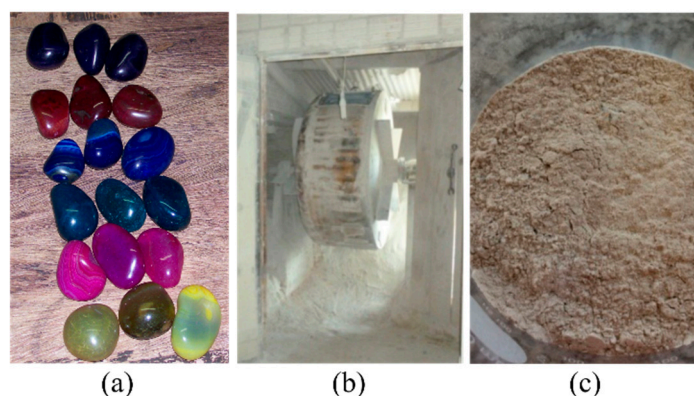


**Figure 1.** (a) Rolled stone, (b) Ball bearing drum and (c) rolled powder.

Hartman et al. [12] claim that the production of agate and amethyst, in the state of Rio Grande do Sul, is approximately 418 tons/month, of which 130 tons/month are processed in Soledade/RS producing more than 6000 pieces/month. This agate processing generates about 80 tons/month of solid waste, that it is usually stored in own company areas that may cause environment damage, such as the waterproofing of soil, rivers contamination, and others.

The reuse of the agate residues as raw material for the manufacture of new products may be an alternative to reduce the use of natural resources. In this sense, the civil construction is an excellent alternative to receive this waste, contributing to the minimization of environmental impacts, since the extraction of raw materials used by this segment generates large impacts, has a high energy consumption, and has a waste generation [13]. For example, these wastes can be used as aggregates replacing the natural sand, which is in scarce in the state of Rio Grande do Sul.

Several studies have been carried out in order to take advantage of the residues produced by precious stone industries in mortars, concretes, and other materials. Petry et al. [11] studied the potential development of alkali-silica reaction in mortars based on different blends agate waste and concluded that the inclusion of powdered agate waste reduces the deleterious effect of alkali-silica reaction, and expansions higher than 0.19% were not identified. Abreu et al. [14] evaluated the feasibility of using the “rolled powder” as mineral addition, noting that the proportion of up to 10% can replace cement, making the concrete produced more sustainable. Venquiarutto et al. [15] verified the addition of agate “rolled powder” as a small aggregate in conventional concretes, and obtained good results against the compressive strength and the absorption of water by capillarity. Betat et al. [16] evaluated the influence of the agate waste as a large aggregate in the compressive strength and cement consumption of concretes produced with different recycled aggregates. Chiaro [17] evaluated agate residue in the average granulometry of sand (average diameter between 0.3 and 1.2 mm) for the production of white and conventional concrete. The results demonstrated that the use of this material as a substitute for natural sand showed deleterious reactions, known as alkali-aggregate

reactions (AAR). In this context, it is shown that the AAR was minimized by adding pozzolanic material as silica fume [11].

The study by Correia [18] evaluated the possibility of replacing natural sand with agate residue in the production of stoneware tile, in the mass proportion of 15 to 45%. The agate powder was also used in the production of ceramics [19], in the development of urban pavement structures [20], as soil remineralizer [21], and in the production of colored sand through magnetite nanoparticle incorporation [22].

Many silica-based wastes have been evaluated to produce efficient cementitious materials such as: self-compacting concrete with waste marble dust [23]; concrete made with granite and marble as recycle aggregates [24]; concrete with high volumes of unprocessed lignite-coal fly ash and rice husk ash [25]; rice husk ash incorporated as a partial replacement for fine aggregate in concrete [26]; concrete produced from coal bottom ash [27]; waste brick as a partial replacement of cement in mortar [28]; concrete from alkali activated slag [29]; waste glass in autoclaved aerated concrete [30]; and, other uses. According to Mehta and Monteiro [31], the concrete can present twenty-seven variations, one of which is lightweight concrete. One type of lightweight concrete is known as aerated concrete, which is normally used in the form of sealing blocks [32], and is divided into aerated foamed concrete blocks (AFCB) and autoclaved aerated concrete blocks (AACB), also known as autoclaved cell concrete blocks (ACCB). AACB in Brazil, is regulated by the Brazilian Association of Technical Standards NBR 13438 [32], and has a specific mass of 400 to 650 kg/m<sup>3</sup>, after hardening.

Though, there is no Brazilian standard for AFCB, but AFCB is internationally standardized. According to the American Society for Testing and Materials, C 495-99a [33,34] the specific mass of Aerated Foamed Concrete (AFC) can range from 320 to 1920 kg/m<sup>3</sup>. The internal structure of foamed concretes includes that of air-voids that form up to 80% of the volume of the material. These small air-voids must be homogeneously distributed within the mortar and are incorporated by adding preformed foam [33,35].

Non-autoclaved lightweight concretes present less compressive strength and greater retraction due to the absence of a curing process when compared to autoclaved ones. This difference is explained by the reactions produced in the autoclave because the materials based on silicon oxide react with calcareous materials and form very well defined structures, known as tobermorite (hydrated calcium silicate—(Ca<sub>5</sub>Si<sub>6</sub>O<sub>16</sub>(OH)<sub>2</sub>·4H<sub>2</sub>O)) [36]. In the curing process in the natural environment, limestone materials initially have an acicular shape and over the first six months are converted into hexagonal calcite crystals [37].

In AFCB, the incorporation of air into the mortar is usually produced by adding preformed foam based on synthetic foam agents. More stable incorporators of air have been sought that reduce the effects of Ostwald ripening, which reduces the coalescence and drainage of the film that encapsulates the air-void. In addition, the study by Krämer et al. [38] demonstrated that adding silica nanoparticles forms emulsions that have a greater strength, thus allowing for a better distribution during mixing in the mortar, thereby improving the stability of the bubbles in the first hours of hydration of the binder. RP has been little explored in the international literature because it is a regional material.

The main aim this paper was to evaluate the use of RP, completely replacing the natural sand in the production of AFCB with a foam agent derived from the fatty acid of coconut. Also, a brief economic and environmental discussion about the use of the agate waste was carried out.

## 2. Materials and Methods

RP was used as aggregate. It was collected in an industry, located in the municipality of Soledade—Rio Grande do Sul, Brazil, that processes rolled agate. The Portland cement (PC) (Cimpasso, Passo Fundo, RS, Brazil) V-ARI used complies with Brazilian standards NBR 5733 [39] and NBR 5737 [40], cements of initial high strength and sulfate tolerance, respectively. The physical and chemical properties of PC and RP are shown in Table 1.

**Table 1.** Physical and chemical properties of Portland Cement (PC) and Rolled Powder (PR).

Physical Properties								
Materials	Specific Gravity g/cm <sup>3</sup>	Blaine Fineness m <sup>2</sup> /kg	Particle Size				pH Paste	
			Pass in 75 µm	D <sub>10%</sub> Mm	D <sub>50%</sub> µm	D <sub>90%</sub> µm		D <sub>average</sub> µm
Portland Cement (PC)	3.1	430	0.5%	1.0	9.6	27.6	12.3	13.0
Rolled Powder (PR)	2.7	80	3.2%	2.8	31.4	151.5	57.6	8.2

Chemical Composition									
Materials	Al <sub>2</sub> O <sub>3</sub>	CaO	CdO	SiO <sub>2</sub>	Fe <sub>2</sub> O <sub>3</sub>	Na <sub>2</sub> O	All Others	SO <sub>3</sub>	Loss on Ignition
Portland Cement (PC)	3.1	60.6	4.3	18.9	0.5	-	13.0	2.0	2.9
Rolled Powder (RP)	1.2	0.4	0.1	92.2	1.1	0.1	0.1	-	3.5

The granulometry of RP was conducted using a Cilas laser granulometer model 1190 (CILAS, ORLEANS, France), with an amplitude of measurement from 0.04 to 2500.00 µm. The chemical composition of the RP was determined by X-ray fluorescence using PANalytical-MiniPal 4 equipment (PANalytical B.V., Almelo, Netherlands) [41]. X-ray diffraction was performed using a Siemens diffractometer model D-500 (Siemens, Monique, Germany), with a Cu anode, set at 40 kV and 17 mA. The 2θ angle was varied from 10–80 degrees, with steps of 0.05 degrees.

The foam-generating mixture consisted of Cocoamidopropyl Betaine (CPB) and Cocamide Diethanolamine (DEA) [42] in a ratio of 1:3 (one part CPB for two parts DEA). This mixture was diluted 1:70 (one part of mixture to sixty-nine of water) to make the pre-made foam.

The foam was prepared by mechanical stirring. The density of the foam formed was 75 kg/m<sup>3</sup>.

The mortar was prepared by mixing the RP, water, cement, and the preformed foam. The constituents of the mortar were stirred by a mechanical stirrer until a homogeneous mass was formed. The AFCB was produced based on the procedures suggested by ASTM C796 and ASTM C869 [43,44].

The designs of experiments to determine the properties of AFCB were developed using the complete factorial statistical method. The experimental design depended on two factors with three and four levels, i.e., the experiments were performed with water/cements (w/c) ratio of 1.08, 1.28, and 1.48; and a foam amount of 14%, 18%, 24% and 28% of the total solid mass (cement mass + RP mass). The amount of aggregate (RP) and binder (cement) were kept constant with equal proportion (1:1). Water levels were adjusted according to variations in the w/c rate. For example, when using 1.0 kg of cement, 1.0 kg of RP, 14% foam and a w/c ratio of 1.08, the amount of water should have been 0.80 kg. Table 2 shows an experimental matrix with 12 concrete traces. Three replicates for each response variable were made to avoid systematic errors.

**Table 2.** Experimental matrix for concrete traces.

Order	w/c Rate	% Foam (of Total Solid Mass)
1	1.08	14
2	1.08	18
3	1.08	24
4	1.08	28
5	1.28	14
6	1.28	18
7	1.28	24
8	1.28	28
9	1.48	14
10	1.48	18
11	1.48	24
12	1.48	28

The samples were demolded after 24 h, packed in plastic film and maintained at a temperature of  $20 \pm 2$  °C for 28 days during the curing time.

The density of the blocks and the specific mass of the RP were determined according to ASTM C138/C138M-16a [45]. The AFCB compression strength tests were performed according to ASTM C495-99a [34], using a universal testing machine (EMIC-PC200C, Instron, Norwood, MA, USA).

An evaluation of the distribution of the air-voids and the form of the particles was performed by secondary electron imaging in a scanning electron microscope (SEM)—Tescan—at 30 kV (Tescan, Kohoutovice, Czech Republic). To measure the bubbles, the samples were prepared according to ASTM C457/C457M-12 [46], and sealed with gold. The images obtained were treated and evaluated using ImageJ software.

Finally, a comparison, related the compressive strength and density between commercial blocks (AFCB and AACB) and AFCB developed with de RP was performed. For this comparison data provided by the manufacturers were used. Also, economic viability was briefly described.

### 3. Results and Discussion

#### 3.1. Characterization of the Rolled Powder (RP)

The results showed that the major constituent of the RP is SiO<sub>2</sub>, at approximately 92.5%. The distribution of the particle size of the RP reveals a granulometry about four times (4×) higher than PC. Due to the absence of amorphous characteristics as measured by the diffractogram, it can be inferred that RP does not present high reactivity when compared to other siliceous materials such as rice husk ash, fly ash, and other biomasses. Table 3 shows that RP has three crystalline phases (quartz, tridymite, and cristobalite), as the cristobalite phases are polymorphic. However, tridymite and cristobalite have a fraction with poor crystallinity, as quantified by the method of Rietveld [47–50]. Furthermore, the quartz phase represents 95% of the sample. The cristobalite phase is 1.5%, cristobalite-*low* at 1.9% and a trydymite-*low* at 1.5%.

**Table 3.** Phase quantification, lattice parameters and crystalline system for Rolled Powder (RP).

Fase	Crystalline System	Lattice Parameters Refined	Quantification	
			% Mass	% Volumetric
Quartzo (SiO <sub>2</sub> )	Trigonal	a = $4.9113 \pm 1.58 \cdot 10^{-4}$ Å c = $5.4016 \pm 2.79 \cdot 10^{-4}$ Å	95.09 ± 0.09	89.03 ± 0.09
Cristobalite-low (SiO <sub>2</sub> )	Tetragonal	a = $5.026 \pm 4.73 \cdot 10^{-4}$ Å c = $6.8446 \pm 2 \cdot 10^{-4}$ Å	1.86 ± 0.12	2 ± 0.12
Tridymite-low (SiO <sub>2</sub> )	Triclinic	a = $5.030 \pm 0.013$ Å b = $9.082 \pm 0.06$ Å c = $8.306 \pm 0.05$ Å α = $91.11 \pm 0.92^\circ$ β = $93.79 \pm 0.48^\circ$ γ = $91.47 \pm 0.81^\circ$	1.54 ± 0.17	7.25 ± 0.17
Cristobalite (SiO <sub>2</sub> )	Cubic	a = $7.1436 \pm 0.0057$ Å	1.5 ± 0.26	1.7 ± 0.26
		Sum	99.99%	99.98%

In the literature [11,15], the agate residue in sand granulometry produces AAR. However, Petry [11] emphasizes that RP reduces the occurrence of AAR by 0.19%. AFCB because it contains empty spaces in its interior, according to Popov et al. [51], can berth expander gel that causes internal tensions and leads to the loss of mechanical resistance. Thus, it is believed that using RP in AFCB may be an interesting possibility, since this may mitigate possible problems related to the use of residues.

SEM was used for the morphological analysis of the residue, and this shows that particles have different sizes as can be seen in Figure 2. These variations may have been generated by the friction

between the parts in the rolling process. It is assumed that the rough grinding process that produces rolled agate has an influence on the modification of the surface of the residue. It is emphasized that the result of the X-ray diffraction (XRD) reinforces this assumption because two phases are identified in which the crystallinity is low.

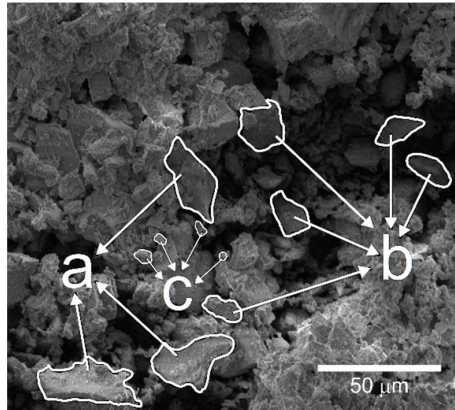


**Figure 2.** Image by scanning electron microscope (SEM) of RP showing the different sizes a-b-c of particles.

### 3.2. Characterization of AFCB

The density was determined following the standards of ASTM C138 [45]. The value of density is a very important parameter because it is directly related to the volume of air incorporated into the mortar and consequently greatly influences the mechanical, thermal, and acoustic characteristics of the blocks [52–54]. In general, if the density is reduced, the compressive strength, the thermal conductivity, and the sound propagation decrease [55,56].

The value of the density is linked to the total volume of the water used in the process. An excess of water breaks the water/foam equilibrium that forms the bubbles. On the other hand, a smaller volume of water reduces the stability of the bubbles because of dehydration [57]. It is observed in Figure 3 that the lower densities occur at the extremes of the compositions (the least and greatest additions of foam). When less foam is added, the air-voids incorporated in the mortar are brought together because of dehydration and form larger bubbles. Similarly, when a greater volume of foam is added, the bubbles rupture because the thickness of the hydrophilic film has been reduced, thereby making them less resistant to the forces of the material medium. However, the results demonstrated that water content changes the interaction between bubbles/mortar and changed the stability of the hydrophilic film of foam [38,53,58].

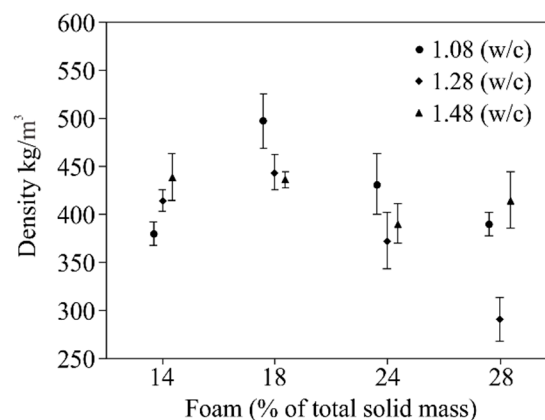


**Figure 3.** Density as a function of foam amount for different w/c rate.

Figures 4 and 5 show the distribution of the air voids and form of the products of hydration (Figure 5: a-b-c), respectively, in the mortar aerated by foam after 28 days of curing. The cavities formed by the bubbles are distributed throughout the area evaluated and are of uniform size, with the maximum diameter being approximately 0.5 mm. The distribution of the pores and the size of the cavity are favored by the low granulometry of the aggregate, thus generating smaller densities. Another interesting aspect is that within the macropores there was a growth of crystals (Figure 5), which is also reported by Mehta and Monteiro [31,38].

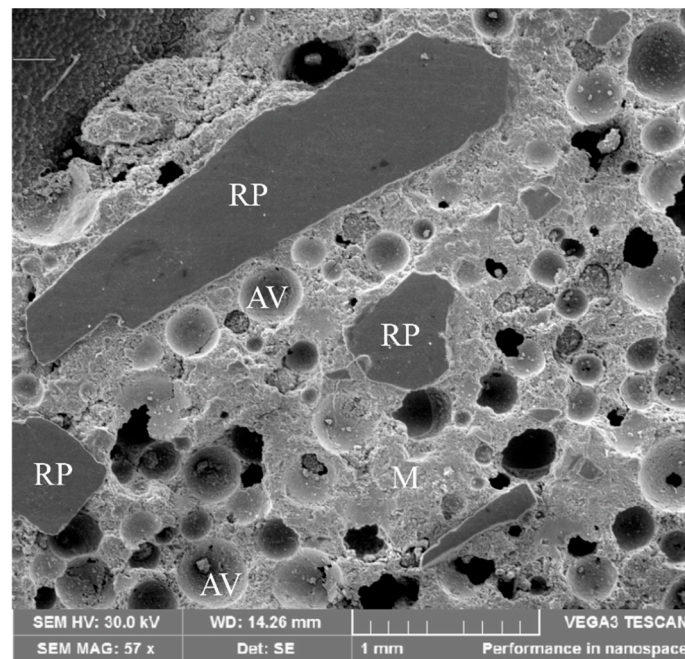


**Figure 4.** SEM of aerated foamed concrete blocks (AFCB) showing the RP grains, air void (AV), and solid matrix (M).

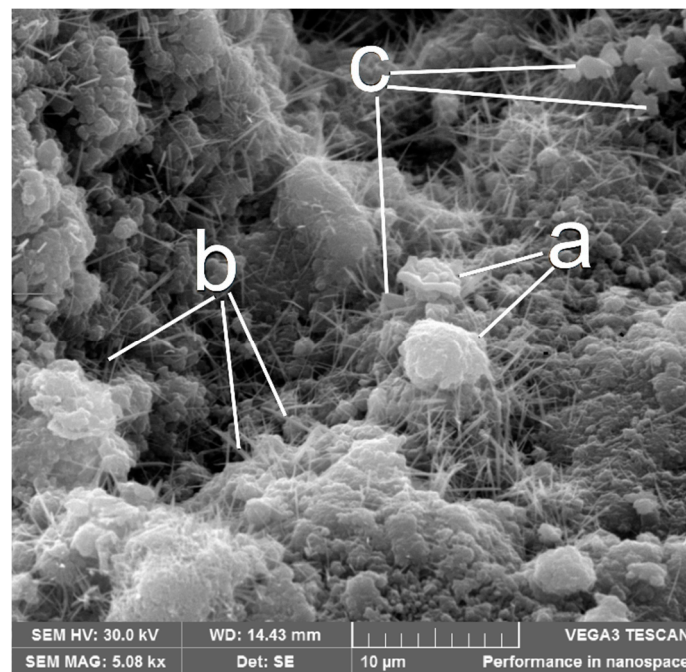


**Figure 5.** SEM of AFCB showing the hydration products in mortar.

The distribution of the pores, the mean diameter, and the area occupied by the air-voids were evaluated using image analysis, namely ImageJ software following Hilal et al. [58]. The results indicate that about 30% of the area is filled with air-voids, the dimensions of which were 0.05 to 0.5 mm, these being defined as macropores by Rouquerol et al. [59]. The pore analysis showed  $D_{10}$  of 90.1  $\mu\text{m}$ ,  $D_{50}$  of 131.2  $\mu\text{m}$ , and  $D_{90}$  of 204.8  $\mu\text{m}$ , and the mean diameter was 264.0  $\mu\text{m}$ . These values are slightly lower than those found by Hilal et al. [58]. However, this difference can be explained by the granulometry of the aggregate. The higher the granulometry of the aggregates, the higher the diameter of the bubbles, whereas the lower the granulometry, the smaller the diameter of the bubbles; moreover, nanoscale particles can form an interfacial layer between the water and the foaming agent, thereby increasing the resistance of the air-voids [38]. The distribution of the macropores is shown in Figure 6.

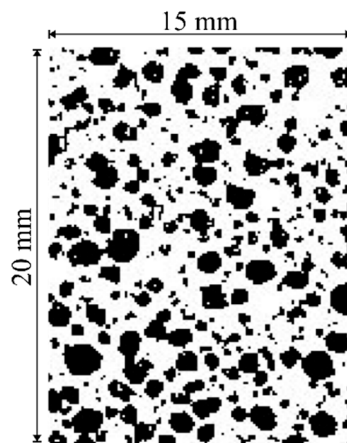


Figure 6. Typical binary images for the sixth mix (Table 2).

Compressive strength was the parameter chosen to define which composition presents the best result, thereby seeking to comply with the Brazilian standard NBR 13438 [32] for ACCB. Figure 7 shows the results of the compressive strength tests. NBR 13438 requires that the compressive strength should have values of at least 1.2 to 1.5 MPa at densities between 400 and 600  $\text{kg}/\text{m}^3$  [32].

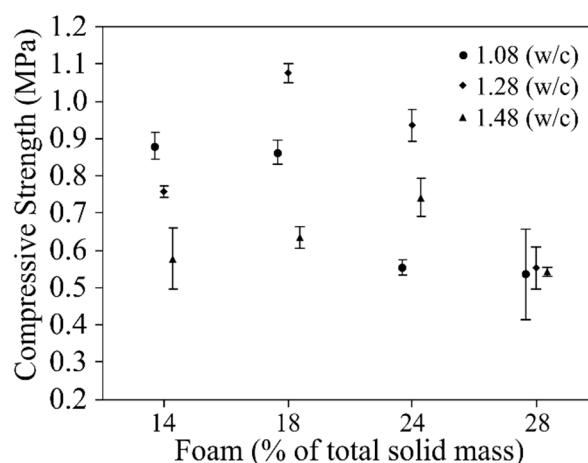


Figure 7. Compressive strength as a function of foam amount for different w/c rates.

In addition to the curing process, the result of the compressive strength is also a function of the density and the physicochemical composition of the mixture. For these tests, the variation of the added foam mass defines what the density and compressive strength will be, since besides



the direct introduction of the air-voids, this leads to an increased water content of the mixture because the preformed foam consists of about 98.6% water. These findings agree with previous works [31,52]. The best value obtained for compressive strength was 1.07 MPa for AFCB with 1.28 w/c and 18% foam (test six—Table 2) by mass added. It was observed that the tests with a w/c of 1.08 did not develop a homogeneous mass prior to adding the preformed foam, due to a lack of hydration. On the other hand, the tests with respect to a w/c of 1.48 showed a high fluidity due to the excess of hydration water.

As observed, the compression strength results are below the limit of the Brazilian standard (NBR 13438), in which the minimum value of compressive strength is 1.2 MPa, but this rule is just for ACCB. These lower results (AFCB) can be explained by the absence of a controlled cure process (autoclave), where the literature states that curing at pressure and temperature produce hydration products from the strongest cements [36,37]. Also, the high amount of cadmium oxide in the cement, generated by the addition of furnace slag in cement manufacture, may have influenced the decrease in compressive strength.

### 3.3. Comparison between Commercial Blocks (AFCB and ACCB) and AFCB Developed with Agate Waste

Table 4 shows the commercial blocks (AFCB and ACCB) and the AFCB of present study characteristics. The difference in the compressive strength between the blocks (commercial and AFCB with RP) is due to density. In the specific case of compressive strength and the density of AFCB, it is believed that production processes, grain size, type of cure, and, mainly, the foam production are factors decisive for its improvement.

**Table 4.** Characteristics of concrete blocks.

Blocks	Compressive Strength (MPa)	Density (kg/m <sup>3</sup> )	Description of Manufacturing Process
Commercial AFCB	2.14	830	water/cement rate of 0.82; 25 kg of natural sand; 25 kg of cement Portland (V-ARI); 20 kg of water; The materials were added in a mixer and stirred for 10 min. Sequentially, 50 liters of foam were added and mixed for another 5 min. The concrete curing was of 28 days in open environment.
Commercial ACCB	4.50	600	Autoclave curing process. Other information not provided by the manufacturer.
Commercial ACCB	1.20	400	Autoclave curing process. Other information not provided by the manufacturer.
AFCB with RP	1.07	430	water/cement rate of 1.28; 500 g of RP; 500 g of cement Portland (V-ARI); 400 g of water; The materials were added in a mixer and stirred for 10 min. Sequentially, 230 g of foam were added and mixed for another 5 min. The concrete curing was of 28 days in open environment.

An economic viability estimate was made by analyzing the production cost of 1 m<sup>3</sup> of commercial AFCB and AFCB with RP. The Table 5 shows the comparative cost between commercial AFCB and AFCB with RP production. In this estimation, the same transportation, electrical energy, and labor costs were considered.

The use of the agate wastes, completely replacing the natural sand, can generate an 18% saving in the AFCB fabrication. This result shows to be promising to use agate wastes in the development of building materials, but an optimization with respect to compressive strength should be performed.

**Table 5.** Comparative production cost of 1 m<sup>3</sup> of AFCB.

Materials	Commercial AFCB Cost (USD)	AFCB with RP Cost (USD)
Cement	45.20	45.20
Natural sand	6.45	0.00
Water	0.40	0.40
Agate waste	0.00	0.00
Commercial foam	5.81	0.00
Foam of study	0.00	1.94
Total cost	57.86	47.54

#### 4. Conclusions

In the present work, AFCB was developed with the addition of RP waste as a substitute aggregate of natural sand. Based on the results and discussion, the following conclusions are made:

- Rolled powder can be used as an aggregate in the manufacture of AFCB, reducing the liabilities of agate manufacturing companies and reducing environmental impacts due to the irregular disposal of this waste. Also, with the use of this residue, it is possible to reduce the consumption of natural sand, which is a finite aggregate and its extraction causes environmental damages, mainly in riverbeds and lakes.
- The results of the RP characterization show that the granulometry and the chemical composition were suitable for the development of AFCB. It is relevant to note that PR was used without any process of beneficiation.
- The concrete blocks showed a microstructure with a mean pore size of 264.0  $\mu\text{m}$ , which is characteristic of this type of material. Also, calcite formation in macropores was found due rate of hydration reactions.
- The w/c ratio and the amount of foam had a significant influence on density and compressive strength. The results for the compressive strength and density of AFCB were slightly lower than those required by ABNT 13438. However, it is important to emphasize that this standard complies with the ACCB, which are autoclaved.
- Overall, the tests enabled the best ratio between PC, RP, water, and foam to be established, which was identified for AFCB with 1.28 of w/c, thus providing the greatest restriction with the lowest density. The w/c ratio set at 1.28 with an addition of 18% foam generated a sample with a density of  $430 \pm 18 \text{ kg/m}^3$ , and a compressive strength about of  $1.07 \pm 0.02 \text{ MPa}$ . This result is close to meeting the requirements of the standard for density classes  $<450 \text{ kg/m}^3$  NBR 13438 [32] for ACCB.
- Economic and financial aspects must be emphasized, since the use of agate waste can significantly reduce the production cost of the companies that generate these wastes. This is because the transportation and environmentally correct costs, today approximately of 55 USD per m<sup>3</sup>, would reduce to zero. Moreover, the AFCB manufacturing cost of using the RP can be 18% less than conventional AFCB cost.

**Acknowledgments:** The two authors (Lermen, R.T. and Silva, R.d.A.) are grateful to the Fundação Meridional for financial support by productivity aid.

**Author Contributions:** Rudimar Pedro and Denisar De Col performed the tests, analyzed results and wrote the paper; Jonas Anversa assisted in the analysis of the results; Rejane M. C. Tubino, Richard Thomas Lermen and Rodrigo de Almeida Silva planned the study, assisted in the analysis of the results and writing the paper.

**Conflicts of Interest:** The authors declare no conflict of interest.

## References

1. Tubino, L.; Sampaio, C. Industrial treatment of raw agate: Spectrocolorimetry and scanning electron microscopy (SEM) analyses. *Dev. Miner. Process.* **2000**, *13*, C1-9–C1-16.
2. Agostini, I.M.; Fiorentini, J.A.; Brum, T.M.M.; Juchem, P.L. *Ágata do Rio Grande do Sul; Série Difusão Tecnológica*; Ministério de Minas e Energia, Departamento Nacional de Produção Mineral: Brasília, Brazil, 1998; No. 5; p. 272.
3. Thomé, A.; Abreu, A.G.D.; Brandli, L.L.; Fernandes, V.M.C.; Prietto, P.D.M. Diagnóstico dos resíduos gerados pelo setor de pedras preciosas do município de Soledade/RS. In *Tecnologias Para o Setor de Gemas, Joias e Mineração*; Hartmann, L.A., Silva, J.T.D., Eds.; Universidade Federal do Rio Grande do Sul/UFRGS: Soledade, Brazil, 2010; Volume 1.
4. Duarte, L.C.; Hartmann, L.A. Geodos preenchidos por ametistas em basaltos da Formação Arapey, Artigas, República Oriental do Uruguai: Modelo Epigenético. In *44 Congresso Brasileiro de Geologia*; Sociedade Brasileira de Geologia: Curitiba, Brazil, 2008.
5. Bossi, J.; Cagianò, W. Contribución a la geología de los yacimientos de ametista del Departamento de Artigas (Uruguai). In *Congreso Brasileiro de Geologia*; Sociedade Brasileira de Geologia: Porto Alegre, Brazil, 1974; Volume 5, pp. 301–318.
6. Heaney, P.J. A proposed mechanism for the growth of chalcedony. *Contrib. Miner. Petrol.* **1993**, *115*, 66–74. [[CrossRef](#)]
7. Brum, T.M.M.; Juchem, P.L.; Fischer, A.C.; Heemann, R.; Castro, J.H.W.; Gouvea, J.C.R., Jr. Características microscópicas da ágata do Salto do Jacuí, RS. In *I Simpósio de Tratamento e Caracterização de Gemas*; Coordenadoria de Imprensa e Editora—UFOP: Ouro Preto, Brazil, 2000.
8. Thomé, A.; Schneider, I.A.; Rosa, F.D.; Consoli, N. Caracterização geotécnica de um resíduo da indústria de pedras semipreciosas e viabilidade de seu uso em estabilização dos solos. In *Congresso Brasileiro de Mecânica dos Solos e Engenharia Geotécnica*; ABMS: São Paulo, Brazil, 2002; Volume 1, pp. 229–240.
9. Vilasbôas, F.; Santos, C.R.D.; Menezes, J.C.S.D.S.; Silva, R.D.A.; Schneider, I.A.H. Environment issues on industrial processing of raw agate. In *Sustainability 16*; Minerals Engineering: Falmouth, UK, 2016.
10. Barros, A.L.; Pizzolato, T.M.; Carissimi, E.; Schneider, I.A.H. Decolorizing dye wastewater from the agate industry with Fenton oxidation process. *Miner. Eng.* **2006**, *19*, 87–90. [[CrossRef](#)]
11. Petry, N.; Masuero, Â.B.; Kirchheim, A.P. Alkali silica reaction in aggregates derived from the valorization of waste from the agate mining. In Proceedings of the 15th International Conference on Alkali-Aggregated Reactions, São Paulo, Brazil, 3–7 July 2016.
12. Hartmann, L.A.; Silva, J.; Tonezer, D. A Porto Alegre: IGEO/UFRGS. In *Tecnologias Para o Setor de Gemas, Joias e Mineração*; Universidade Federal do Rio Grande do Sul—UFRGS: Porto Alegre, Brazil, 2010.
13. Petry, N.D.S. *Uso de Resíduos de Ágata Como Agregado em Argamassas de Cimento Portland Branco*; Programa de Pós-Graduação em Engenharia Civil; Universidade Federal do Rio Grande do Sul: Porto Alegre, Brazil, 2015.
14. Abreu, A.G.D.; Silveira, A.A.; Santos, T.M. Pó de resíduos de ágata como adição mineral. In Proceedings of the V Congresso Internacional 19a Reunión Técnica “Ing. Oscar R. Batic”, Buenos Aires, Argentina, 7–9 November 2012; Volume 1, pp. 55–62.
15. Venquiaruto, S.; Ossorio, A.; I, C.Z.; Passuelo, A.; Kirchheim, A.P.; Dalmolin, D.C.C.; Massuero, A. Aproveitamento de resíduos de ágata reciclada em materiais cimentícios sustentáveis. In *Tecnologia e Inovação em Gemas, Joias e Mineração*; Hartmann, L., Silva, J.T.D., Eds.; Universidade Federal do Rio Grande do Sul: Porto Alegre, Brazil, 2014; Volume 1.
16. Betat, E.F.; Pereira, F.M.; Verney, J.C.K. Concretos produzidos com resíduos do beneficiamento de ágatas: Avaliação da resistência a compressão e do consumo de cimento. *Rev. Matér.* **2009**, *14*, 10. [[CrossRef](#)]
17. Chiaro, S.M.X. *Reação Alkali-Agregado em Concretos Brancos com Agregados de Miúdos de Reciclados de Ágata*; Universidade Federal do Rio Grande do Sul—UFRGS: Porto Alegre, Brazil, 2012.
18. Correia, S.L.; Dienstmann, G.; Folgueras, M.V.; Segadaes, A.M. Effect of quartz sand replacement by agate rejects in triaxial porcelain. *J. Hazard. Mater.* **2009**, *163*, 315–322. [[CrossRef](#)] [[PubMed](#)]
19. Pereira, B.V.; Basegio, T.; Vilanova, D.L.; Bergmann, C.P. Beneficiamento de ágata para a preparação de Materiais Cerâmicos. In *Seminário de Iniciação Científica*; Universidade Federal do Rio Grande do Sul—UFRGS: Porto Alegre, Brazil, 2014.

20. DallaRosa, F.; Thomé, A.; Donato, M. Análise da viabilidade técnica da aplicação do resíduo da rolagem de pedras preciosas em estruturas de pavimentos urbanos. In *Tecnologia e Inovação em Gemas, Joias e Mineração*; Hartmann, L.A., Silva, J.T.D., Donato, M., Eds.; Instituto de Geociências UFRGS: Porto Alegre, Brazil, 2014; Volume 1, pp. 83–94.
21. Donato, M.; Bortoluzzi, E.C.; Abreu, C.T.; DallaRosa, F. Transformação de resíduos da mineração para uso como artefato de concreto e remineralizador de solo. In *Inovação, Design e Pesquisas Aplicadas em Gemas, Joias e Mineração*; Donato, M., Duarte, L.d.C., Hartmann, L.A., Eds.; Instituto de Geociências UFRGS: Porto Alegre, Brazil, 2015; Volume 1, pp. 90–96.
22. Folle, D.; Silva, R.D.A.; Boita, J.; Carissimo, D.; Schneider, I.A.H. Waste generation in Agate processing: Use of SiO<sub>2</sub> as a support matter for Fe<sub>3</sub>O<sub>4</sub>. *Int. J. Civ. Struct. Eng.* **2015**, *2*, 327–331.
23. Topçu, İ.B.; Bilir, T.; Uygunoğlu, T. Effect of waste marble dust content as filler on properties of self-compacting concrete. *Constr. Build. Mater.* **2009**, *23*, 1947–1953. [[CrossRef](#)]
24. Binici, H.; Shah, T.; Aksogan, O.; Kaplan, H. Durability of concrete made with granite and marble as recycle aggregates. *J. Mater. Process. Technol.* **2008**, *208*, 299–308. [[CrossRef](#)]
25. Sua-iam, G.; Makul, N. Utilization of high volumes of unprocessed lignite-coal fly ash and rice husk ash in self-consolidating concrete. *J. Clean. Prod.* **2014**, *78*, 184–194. [[CrossRef](#)]
26. Kunchariyakun, K.; Asavapisit, S.; Sombatsompop, K. Properties of autoclaved aerated concrete incorporating rice husk ash as partial replacement for fine aggregate. *Cem. Concr. Compos.* **2015**, *55*, 11–16. [[CrossRef](#)]
27. Kurama, H.; Topçu, İ.B.; Karakurt, C. Properties of the autoclaved aerated concrete produced from coal bottom ash. *J. Mater. Process. Technol.* **2009**, *209*, 767–773. [[CrossRef](#)]
28. Naceri, A.; Hamina, M.C. Use of waste brick as a partial replacement of cement in mortar. *Waste Manag.* **2009**, *29*, 2378–2384. [[CrossRef](#)] [[PubMed](#)]
29. Esmaily, H.; Nuranian, H. Non-autoclaved high strength cellular concrete from alkali activated slag. *Constr. Build. Mater.* **2012**, *26*, 200–206. [[CrossRef](#)]
30. Walczaka, P.; Małolepszyb, J.; Rebenb, M.; Szymański, P.; Rzepa, K. Utilization of waste glass in autoclaved aerated concrete. *Procedia Eng.* **2015**, *122*, 302–309. [[CrossRef](#)]
31. Mehta, P.K.; Monteiro, P.J.M. *Concrete: Microstructure, Properties, and Materials*, 4th ed.; McGraw Hill Professiona’s Access Engineering: New York, NY, USA, 2014.
32. Associação Brasileira Normas Tecnicas (ABNT). *NBR13438—Blocos de Concreto Celular Autoclavado-Requisitos*; Associação Brasileira Normas Tecnicas: Rio de Janeiro, Brazil, 2013; p. 5.
33. Fouad, F.H. *Significance of Tests and Properties of Concrete and Concrete-Making Materials, STP 169D*; Lamond, J.F., Pielert, J.H., Eds.; American Society for Testing and Materials International: Bridgeport, NJ, USA, 2006; pp. 561–569.
34. American Society for Testing and Materials (ASTM) International. *C495-99a—Standard Test Method for Compressive Strength of Lightweight Insulating Concrete*; American Society for Testing and Materials International: West Conshohocken, PA, USA, 1999.
35. Narayanan, N.; Ramamurthy, K. Structure and properties of aerated concrete: A review. *Cem. Concr. Compos.* **2000**, *22*, 321–329. [[CrossRef](#)]
36. Ferreira, O.A.R. *Concreto Celulares Espumosos*; Boletim Técnico do Departamento de Engenharia Construção Civil; Escola Politécnica da Universidade de São Paulo: São Paulo, Brazil, 1987.
37. Wongkeo, W.; Chaipanich, A. Compressive strength, microstructure and thermal analysis of autoclaved and air cured structural lightweight concrete made with coal bottom ash and silica fume. *Mater. Sci. Eng. A* **2010**, *527*, 3676–3684. [[CrossRef](#)]
38. Krämer, C.; Schauerte, M.; Kowald, T.L.; Trettin, R.H.F. Three-phase-foams for foam concrete application. *Mater. Charact.* **2015**, *102*, 173–179. [[CrossRef](#)]
39. Associação Brasileira Normas Tecnicas (ABNT). *NBR 5733/91 (EB 2)—Cimento Portland de Alta Resistência Inicial*; Associação Brasileira Normas Tecnicas: Rio de Janeiro, Brazil, 1991.
40. Associação Brasileira Normas Tecnicas (ABNT). *NBR 5737—Cimentos Portland Resistentes a Sulfatos*; Associação Brasileira Normas Tecnicas: Rio de Janeiro, Brazil, 1992.
41. Paiva, M.P.D. *Caracterização e Flotação de Minérios de Fosfato da Mina de Sofia-Chile*; Universidade Federal do Rio Grande do Sul: Porto Alegre, Brazil, 2012.

42. Oliveira, C.H.; Binotti, R.S.; Barrientos-Astigarraga, R.E.; Graudenz, G.S.; Neto, A.C. Surfactantes derivados do fruto de coco (*Cocos nucifera* L.) e sensibilidade cutânea. *Rev. Bras. Alerg. Immunopatol.* **2005**, *28*, 155–160.
43. American Society for Testing and Materials (ASTM) International. *ASTM C796/C796M-12—Standard Test Method for Foaming Agents for Use in Producing Cellular Concrete Using Preformed Foam*; American Society for Testing and Materials International: West Conshohocken, PA, USA, 2012.
44. American Society for Testing and Materials (ASTM) International. *C869/C869M-11—Standard Specification for Foaming Agents Used in Making Preformed Foam for Cellular Concrete*; American Society for Testing and Materials International: West Conshohocken, PA, USA, 2016.
45. American Society for Testing and Materials (ASTM) International. *C138/C138M-16a—Standard Test Method for Density (Unit Weight), Yield, and Air Content (Gravimetric) of Concrete*; American Society for Testing and Materials International: West Conshohocken, PA, USA, 2016.
46. American Society for Testing and Materials (ASTM) International. *C457/C457M-12—Standard Test Method for Microscopical Determination of Parameters of the Air-Void System in Hardened Concrete*; American Society for Testing and Materials International: West Conshohocken, PA, USA, 2012.
47. Will, G.; Bellotto, M.; Parrish, W.; Hart, M. Crystal structures of quartz and magnesium germanate by profile analysis of synchrotron-radiation high-resolution powder data. *J. Appl. Crystallogr.* **1988**, *21*, 182–191. [[CrossRef](#)]
48. Barth, T.F.W. The cristobalite structures. *Am. J. Sci.* **1932**, *136*, 350–356. [[CrossRef](#)]
49. Graetsch, H.A. Modulated crystal structure of incommensurate low tridymite. *Acta Crystallogr. Sect. B Struct. Sci.* **2009**, *65*, 543–550. [[CrossRef](#)] [[PubMed](#)]
50. Dollase, W. Reinvestigation of the structure of low cristobalite. *Z. Kristallogr. Cryst. Mater.* **1965**, *121*, 369–377. [[CrossRef](#)]
51. Popov, M.; Zakrevskaya, L.; Vaganov, V.; Hempel, S.; Mechtcherine, V. Performance of lightweight concrete based on Granulated Foamglass. In *2nd International Conference on Innovative Materials, Structures and Technologies, Materials Science and Engineering*; IOP Publishing Ltd.: Bristol, UK, 2015.
52. Alexanderson, J. Relations between structure and mechanical properties of autoclaved aerated concrete. *Cem. Concr. Res.* **1979**, *9*, 507–514. [[CrossRef](#)]
53. Ramamurthy, K.; Kunhanandan Nambiar, E.K.; Indu Siva Ranjani, G. A classification of studies on properties of foam concrete. *Cem. Concr. Compos.* **2009**, *31*, 388–396. [[CrossRef](#)]
54. Zhang, Z.; Provis, J.L.; Reid, A.; Wang, H. Geopolymer foam concrete: An emerging material for sustainable construction. *Constr. Build. Mater.* **2014**, *56*, 113–127. [[CrossRef](#)]
55. Laukaitis, A.; Fiks, B. Acoustical properties of aerated autoclaved concrete. *Appl. Acoust.* **2006**, *67*, 284–296. [[CrossRef](#)]
56. Amran, Y.H.M.; Farzadnia, N.; Abang Ali, A.A. Properties and applications of foamed concrete: A review. *Constr. Build. Mater.* **2015**, *101*, 990–1005. [[CrossRef](#)]
57. Secco, M.P.; Tiecher, C.; Ribeiro, B.P.; Santos, T.J.P.D.; Meira, C.; Silva, M.D.; Silva, R.D.A. Obtenção de bloco de concreto celular como tema gerador para ensino médio. *Rev. Eng. Civ. IMED* **2015**, *2*, 35–43. [[CrossRef](#)]
58. Hilal, A.A.; Thom, N.H.; Dawson, A.R. Failure mechanism of foamed concrete made with/without additives and lightweight aggregate. *J. Adv. Concr. Technol.* **2016**, *14*, 511–520. [[CrossRef](#)]
59. Rouquerol, J.; Avnir, D.; Fairbridge, C.W.; Everett, D.H.; Haynes, J.H.; Pernicone, N.; Ramsay, J.D.F.; Sing, K.S.W.; Unger, K.K. Recommendations for the characterization of porous solids. *Pure Appl. Chem.* **1994**, *66*, 1739–1758. [[CrossRef](#)]

